



UNIVERSITÀ
DEGLI STUDI
FIRENZE

FLORE

Repository istituzionale dell'Università degli Studi di Firenze

Pediatric rhabdoid meningioma: a morphological, immunohistochemical, ultrastructural and molecular case study.

Questa è la Versione finale referata (Post print/Accepted manuscript) della seguente pubblicazione:

Original Citation:

Pediatric rhabdoid meningioma: a morphological, immunohistochemical, ultrastructural and molecular case study / Buccoliero AM; Castiglione F; Rossi Degl'Innocenti D; Franchi A; Sanzo M; Cetica V; Giunti L; Sardi I; Mussa F; Giordano F; Genitori L; Taddei GL.. - In: NEUROPATHOLOGY. - ISSN 0919-6544. - STAMPA. - 31:(2011), pp. 59-65.

Availability:

This version is available at: 2158/645744 since:

Terms of use:

Open Access

La pubblicazione è resa disponibile sotto le norme e i termini della licenza di deposito, secondo quanto stabilito dalla Policy per l'accesso aperto dell'Università degli Studi di Firenze (<https://www.sba.unifi.it/upload/policy-oa-2016-1.pdf>)

Publisher copyright claim:

(Article begins on next page)

Case Report

Pediatric rhabdoid meningioma: a morphological, immunohistochemical, ultrastructural and molecular case study

**Anna Maria Buccoliero,¹ Francesca Castiglione,² Duccio Rossi Degl'Innocenti,²
Alessandro Franchi,² Massimiliano Sanzo,³ Valentina Cetica,⁴ Laura Giunti,⁵ Iacopo Sardi,⁴
Federico Mussa,³ Flavio Giordano,³ Lorenzo Genitori³ and Gian Luigi Taddei²**

¹Department of Biomedicine, Careggi Hospital, ²Department of Human Pathology and Oncology, University of Florence, Divisions of ³Neurosurgery, ⁴Oncoematology and ⁵Medical Genetic, Anna Meyer Children's Hospital, Florence, Italy

Rhabdoid meningioma is an uncommon meningioma variant categorized as WHO grade III. The majority of cases occur in adulthood. Herein, we describe a right fronto-temporal rhabdoid meningioma affecting a 3-year-old boy. The lesion measured approximately 4 cm in diameter and incorporated the ipsilateral middle cerebral artery. Sub-total surgical excision of the mass was performed. Histologically, the tumor was mainly composed of globoid plump cells with inclusion-like eosinophilic cytoplasm, peripheral nuclei, prominent nucleoli and occasional intra-nuclear cytoplasmic pseudo-inclusion. The cells appeared in many areas loosely arranged and focally disclosed a papillary architecture. At immunohistochemistry, the tumor cells were EMA, vimentin, HHF35, PgR, INI-1 and p53 positive. The proliferative index (Mib-1) was 15% in the most positive areas. Ultrastructurally, tumoral cells showed an abundant cytoplasm, which was filled with numerous intermediate filaments. Desmosomal junctions were seen. RT-PCR revealed the presence of *NF2* gene expression. Molecular study did not indicate alterations of the *INI-1* gene, whereas it showed the presence of Pro72Arg in exon 4 at heterozygous state in the *TP53* gene. Morphologic features along with immunohistochemical, ultrastructural and molecular results were consistent with the diagnosis of rhabdoid meningioma. The patient was treated with chemotherapy. The lesion remained stable after 33 months of follow-up. Rhabdoid meningiomas rarely occur in children. Owing to its rarity, each new case

should be recorded to produce a better clinical, pathological, molecular, prognostic and therapeutic characterization of this lesion.

Key words: brain, central nervous system, meningioma, pediatric, rhabdoid.

INTRODUCTION

Brain tumors are the most common solid malignancies in childhood. A wide spectrum of primary brain tumors that differ in etiology, morphology, response to radiotherapy or chemotherapy and prognosis, may arise in the pediatric age group. However, childhood meningiomas are infrequent. The majority of them occur in the setting of particular risk factors, including neurofibromatosis type 2 syndrome and prior radiation.¹

Herein, we describe a rare case of rhabdoid meningioma affecting a 3-year-old boy. The morphological, immunohistochemical, ultrastructural and molecular (*TP53*, *NF2*, *INI-1*) traits of this tumor are described.

CLINICAL HISTORY

A 3-year-old boy, with a recent history of seizures, was admitted to the Neurosurgery Unit of the Meyer Children's Hospital. He was the full-term result of a normal pregnancy. Family history was unremarkable. Neurocutaneous stigmata were absent. His weight was 17 kg and his cranial circumference was 50 cm. There were no neurological focal deficits or signs and symptoms of cranial hypertension. CT scan and MRI showed a right fronto-temporal inhomogeneous, hypervascularized and calcified mass measuring approximately 4 cm in diameter. It involved the

Correspondence: Anna Maria Buccoliero, MD, PhD, Department of Biomedicine, Careggi Hospital, Florence, V.le GB. Morgagni, 85, 50134 Florence, Italy. Email: ambuccoliero@unifi.it

Received 6 August 2009; revised and accepted 18 February 2010.

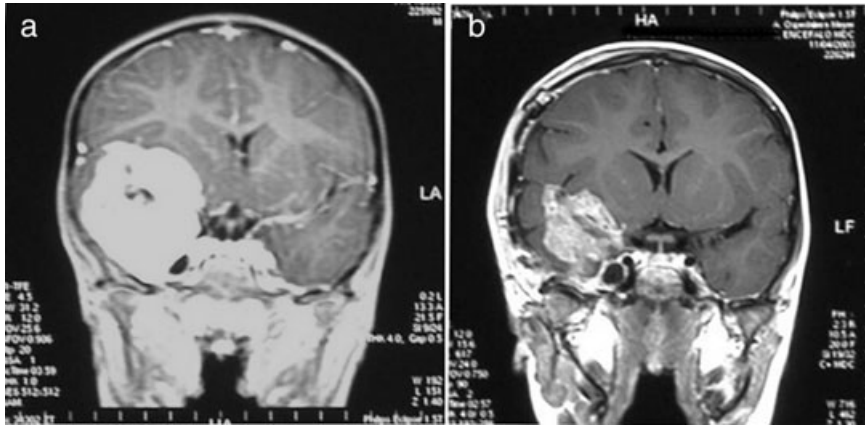


Fig. 1 Preoperative MRI (gadolinium – Gd-TPA – contrast medium) coronal section: middle cranial fossa mass in conjunction with the dura mater extending into the sylvian fissure (a). Postoperative MRI (gadolinium – Gd-TPA – contrast medium) coronal section: residual tumor in the sylvian fissure with contiguous middle cerebral artery (b).

orbital fissure and the lesser sphenoidal wing and entirely occupied the temporal fossa incorporating the ipsilateral middle cerebral artery. The lesion determined mass effect with consequent midline shift and was accompanied by basal hyperostosis (Fig. 1a). A right pterional craniotomy was performed. During surgery the mass, which arose from the meninges, appeared not well demarcated from the perilesional parenchyma, particularly in the sylvian area. Post-surgical radiological studies showed a sub-total excision (Fig. 1b). Due to the absence of any consolidated therapy for pediatric rhabdoid meningioma and in consideration of the young age, the patient was treated with chemotherapy (ICE: ifosfamide, carboplatin and etoposide). The therapy was tolerated well. At revaluations the child achieved radiological and clinical stabilization for a period of 33 months.

METHODS

Optic microscopy and immunohistochemistry

The surgical specimen was fixed in 10% buffered neutral formalin and embedded in paraffin. Some 5 µm sections were stained with HE for the morphological evaluation, whereas further 5 µm sections of the most representative specimen were mounted on electrostatic slides and used for the immunohistochemical studies. Immunohistochemical studies were performed using the standard streptavidin-biotin technique and commercially available reagents (epithelial membrane antigen, EMA, clone E29: DAKO CYTOMATION, Glostrup, Denmark; vimentin, VIM, clone V9: Bio-Genex, San Ramon, CA, USA; GFAP, clone ZCG29: Zymed Laboratory, San Francisco, CA, USA; S-100 protein, polyclonal: DAKO CYTOMATION; smooth muscle actin, clone 1A4: Cell Marque Corporation, Rocklin, CA, USA; muscle-specific actin, clone HHF35: Cell Marque; synaptophysin, SP, polyclonal: Cell Marque; neurofilaments, NF, clone 2F11: Cell Marque; desmin, clone

DE-R-11: Ventana Medical Systems, Tucson, AZ, USA; cytokeratins, clone AE1: Ventana; clone AE3: Ventana; clone CAM 5.2: BD Biosciences, Becton Dickinson, San Jose, CA, USA; estrogen and progesterone receptors, ER, clone D15: Bio-Genex; PgR, clone 1A6: Bio-Genex; p53, clone DO-7: Ventana; BAF47, INI-1, clone 25/BAF47: BD Biosciences, Chicago, IL, USA; and Ki-67, clone Mib-1: DAKO CYTOMATION.

Electron microscopy

Tissue for electron microscopy was obtained from the paraffin block, post-fixed in osmium tetroxide, dehydrated in graded ethanol, embedded in epoxy resin, and cut with a diamond knife in a Leica Ultracut R microtome (Leica Microsystems, Wien, Austria). Ultrathin sections were stained with uranyl acetate and lead citrate, and viewed with a Philips 410 LS transmission electron microscope (Philips' Gloeilampenfabrieken, Eindhoven, Netherlands).

RT-PCR and gene sequencing

From the fresh surgical specimen we selected a fragment macroscopically representative of the tumor. Successively, we cut it in half: from one half several 5-µm frozen sections stained with HE were obtained to verify the adequacy of the specimen (presence of pathological tissue only); the other half was immersed in RNAlater™ (QIAGEN, Valencia, CA, USA) and was kept overnight at +4°C and finally stored at –80°C until analysis.

RNA isolation and real time-PCR

RNA was isolated from 5 mg tissue using 6100 Nucleic Acid PrepStation (Applied Biosystems, Foster City, CA, USA). RNA fragmentation state was evaluated by 1.5% agarose gel. All RNA (200 ng) was reverse-transcribed to cDNA using iScript cDNA Synthesis Kit (Biorad, Hercules, CA, USA). TaqMan real-time quantitative PCR was

performed on an ABI PRISM 7000 Sequence Detector System (Applied Biosystems). PCR product for *NF2* and *GAPDH* genes was detected using gene-specific primers and probes (Applied Biosystems).

Mutation analysis

Genomic DNA from blood and tumor tissue were extracted with QIAamp DNA Kit (QIAGEN, Milan, Italy) according to the manufacture's protocol and DNA concentrations were determined using spectrophotometer GeneQuant II (Pharmacia, Cambridge, UK).

PCR amplifications of the complete coding sequence and flanking exon-intron borders of the *INI-1* (exons 1–9) and *TP53* (exons 2–11) were performed under standard conditions using HotStarTaq DNA Polymerase (QIAGEN, Milan, Italy). The sequencing reactions were performed by means of BigDye Terminator v1.1 Cycle Sequencing Kit (Applied Biosystems). Products of the sequencing reaction were run and analyzed with the ABI Prism® 3130 Genetic Analyzer (Applied Biosystems).

Microsatellite analysis

We analyzed seven polymorphic microsatellite repeat markers (D22S257, D22S427, D22S311, D22S1154, D22S1174, D22S277, D22S1170) labeled with NED (<http://www3.appliedbiosystems.com>) to evaluate loss of heterozygosity (LOH) on chromosome 22 (22q). Amplification was performed with 50 ng of genomic DNA from normal and tumor tissue. Products were run on an ABI PRISM 310 Genetic Analyzer (Applied Biosystems) and analyzed with GeneScan and Genotyper softwares (Applied Biosystems).

RESULTS

The lesion was mainly (more than 50%) composed of a proliferation of globoid plump cells with inclusion-like eosinophilic cytoplasm, peripheral nuclei, prominent nucleoli and occasional intra-nuclear cytoplasmic pseudo-inclusions. The cells appeared in many areas rather loosely arranged and sometimes disclosed a papillary architecture. In some areas, the lesion was constituted of spindle-shaped cells and the interstitial space contained collagen bundles. Focally, an organoid architectural pattern was also observed (isles of spindle-shaped or globoid plump cells delimited by smaller cuboidal cells) (Fig. 2a–e). There were no whorls or psammoma bodies. Mitotic index ranged from 0–5 per 10 high-power fields. Hemorrhages and vascular hyperplasia were evident. Focal areas of necrosis were also present.

By immunohistochemical staining, the tumor cells were EMA, VIM and p53 positive and GFAP, SP, NF, NSE, 1A4,

desmin, AE1/AE3, CAM5.2 and ER negative. S-100, HNF35 and PgR were focally positive. Furthermore, the tumor cells exhibited diffuse INI-1 nuclear staining. The proliferative index, determined by estimating the percentage of the Mib-1 positive neoplastic cells in the total tumoral cells in the most positive areas, was 15% (Fig. 3a–c).

Ultrastructurally, neoplastic cells showed a round to oval shape with peripherally located nucleus and abundant cytoplasm, which was filled with numerous intermediate filaments and contained few organelles, including rough endoplasmic reticulum profiles, Golgi cisternae, and a small amount of mitochondria. Desmosomal junctions between adjacent cells were seen (Fig. 4).

The RT-PCR revealed the presence of *NF2* gene expression in the tissue sample.

Molecular analysis of *INI-1* gene did not show any variation in sequence or LOH at D22S257, D22S1154, D22S1174, D22S277 and D22S1170 loci. D22S427 and D22S311 were not informative. *TP53* gene analysis showed the presence of Pro72Arg in exon 4 at the heterozygous state (Fig. 5).

Morphologic features along with immunohistochemical, ultrastructural and molecular results were consistent with the diagnosis of rhabdoid meningioma.

DISCUSSION

Meningiomas are frequent primary intracranial neoplasms (approximately 25% of all primary tumors in this site) arising from the leptomeningeal covering of the CNS. They predominantly affect middle-aged and elderly women. Radiation exposure, hormonal and genetic factors play a role in their development and growth. Meningiomas are usually sporadic but may also be a manifestation of the hereditary syndrome neurofibromatosis type 2, which is characterized, at the nervous system level, by the development of schwannomas, meningiomas, ependymomas, and occasionally, gliomas and neurofibromas. The World Health Organization (WHO) recognizes three histological meningioma grades (WHO I or benign, WHO II or atypical, and WHO III or anaplastic) with an increasing risk of recurrence and unfavorable outcome. Recurrence rates of 7–20%, 29–40% and 50–70% are reported, respectively, for benign WHO I, atypical WHO II, and anaplastic WHO III meningiomas. Meningiomas exhibit a wide range of histological patterns with numerous classified subtypes and several uncategorized subtypes. In most cases histological variants do not have prognostic significance. However, clear cell, chordoid, papillary and rhabdoid meningiomas are clinically aggressive.^{2–4} Meningiomas are rare in the pediatric population. Indeed, although tumors of the CNS are the second most common neoplasms in children,

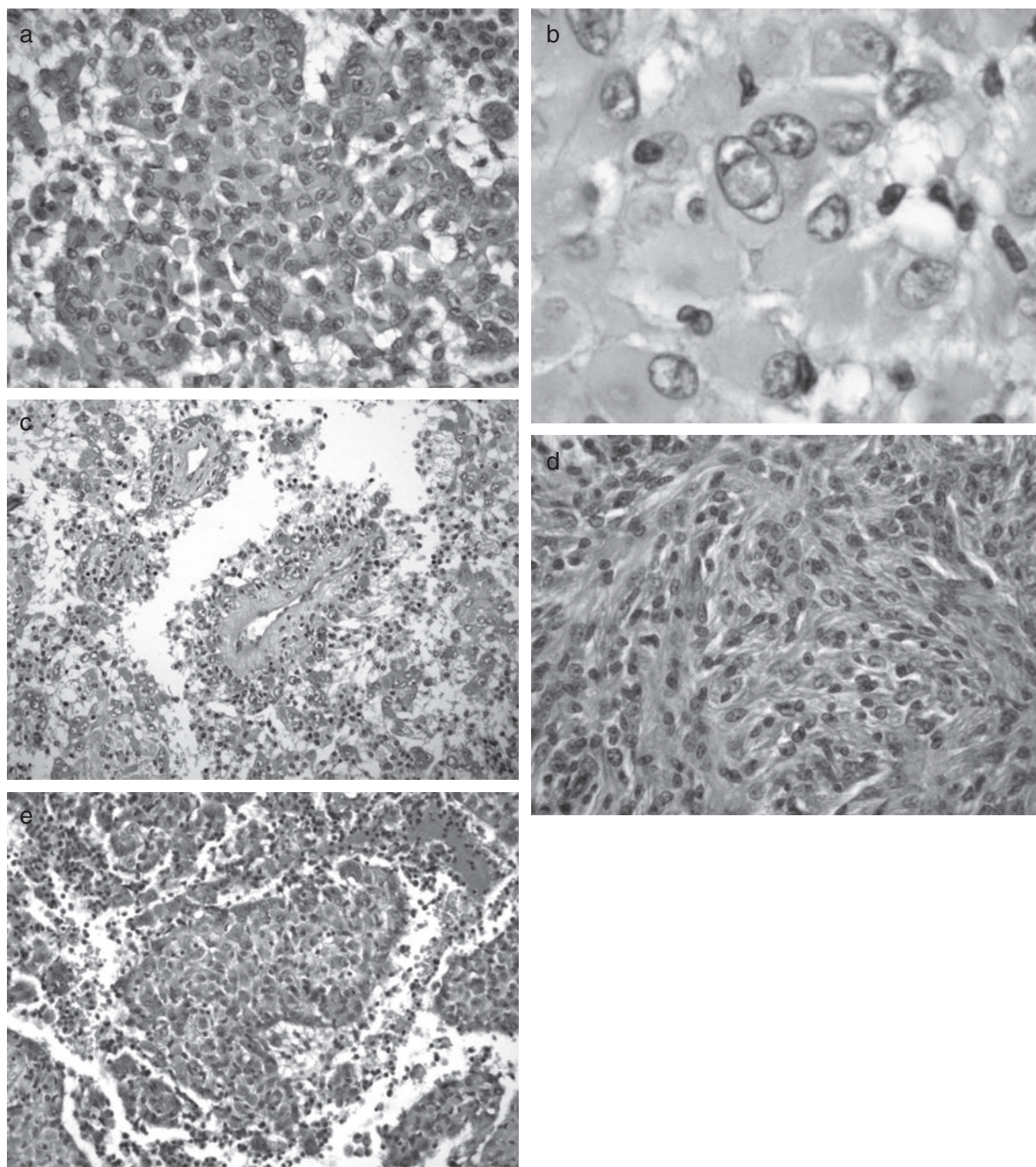


Fig. 2 Globoid and loosely arranged tumoral cells showing an eosinophilic ample hyaline cytoplasm, peripheral nuclei, prominent nucleoli (a) and occasional intra-nuclear cytoplasmic pseudo-inclusions (b); papillary architecture (c); spindle-shaped cells (d); organoid architectural pattern (isle of globoid cells delimited by smaller cuboidal cells) (e). HE; original magnification: a, c–e $\times 200$; b $\times 400$.

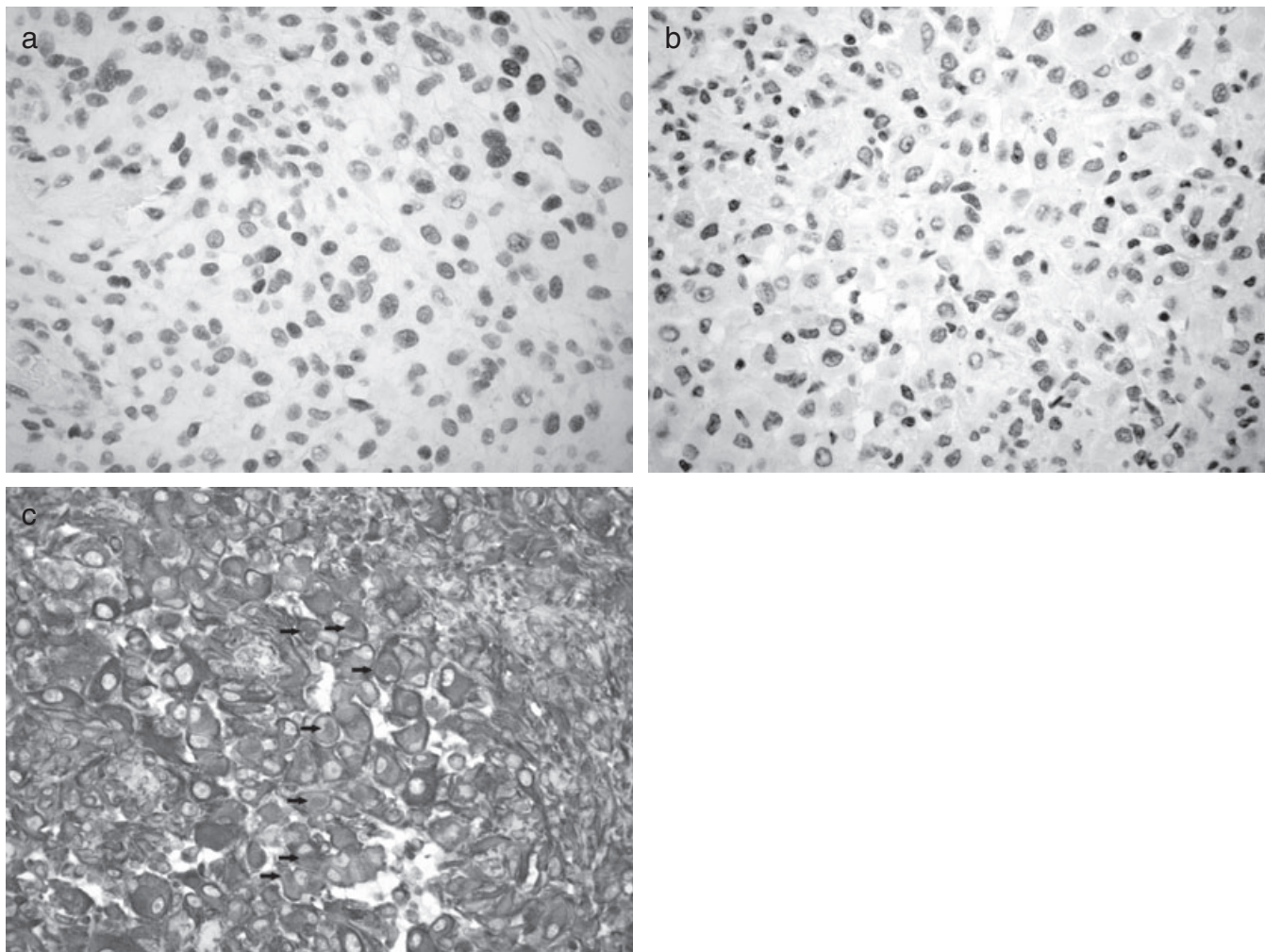


Fig. 3 p53 (a), INI-1 (b) and vimentin (VIM) (c) immunostaining; whorled intermediate filaments which are VIM-positive are visible (the arrows indicate some of them) (c). Original magnification: a–c $\times 200$.

intracranial meningiomas account for only 1% to 4.2% of all brain tumors in this age group.^{5,6}

Rhabdoid meningioma is an uncommon meningioma variant composed of plump cells with abundant eosinophilic fibrillary to hyaline cytoplasm, eccentric nuclei and prominent nucleoli. The majority of the cases have a high proliferative index and other histological features of malignancy. Some cases combine the features of the papillary and rhabdoid types. Rhabdoid meningiomas often undergo an aggressive clinical course and are categorized as WHO grade III. Nevertheless, a minority of rhabdoid meningiomas show inconspicuous histological features of malignancy. The behavior of these cases remains to be determined.⁴ The majority of rhabdoid meningiomas occur in adulthood. In fact, only 11 juvenile cases have been reported in the international literature (the majority of these patients, 6/11, 55%, were teenagers; only 2, 18%, were preschool children). Adjuvant therapy is considered essen-

tial in the management of rhabdoid meningiomas. The outcome of the few reported juvenile rhabdoid meningiomas seems to be better than their adult counterparts. In fact, in the group of 11 juvenile reported rhabdoid meningiomas, there was only one recurrence (4 months after the surgery) and one death (25 years after the surgery).^{7–12} Nevertheless, the small number of reported pediatric rhabdoid meningiomas makes conclusive prognostic remarks difficult.

In our patient the disease is stable 33 months after the diagnosis. This datum could confirm the hypothesis that rhabdoid meningioma has a relatively less aggressive behavior in children.¹² On the other hand, the present case showed alterations in the p53 protein and *TP53* gene (p53 over-expression and *TP53* alteration – Pro72Arg variation allele). The p53 has been shown to be an important protein, associated with cell cycle control, cell differentiation, maintenance of genomic stability, senescence and apoptosis. Therefore, its inactivation is generally regarded as an

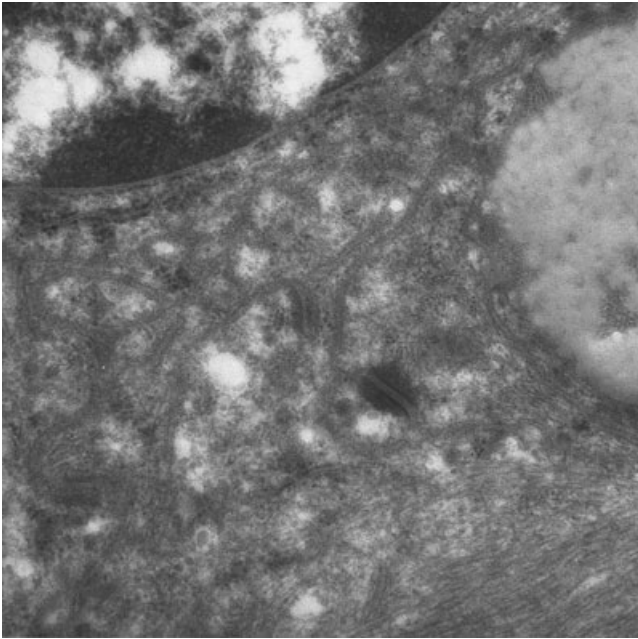


Fig. 4 Electron microscopy: numerous intermediate filaments and desmosomal junctions between adjacent cells. Original magnification: $\times 21\,000$.

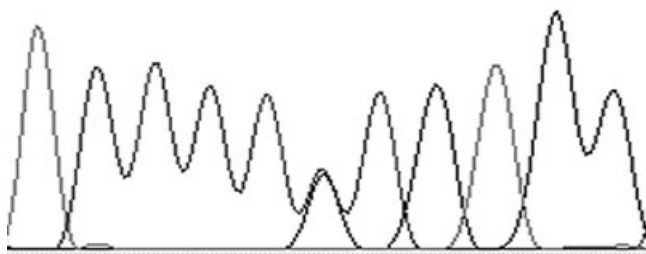
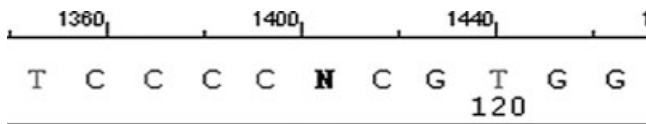


Fig. 5 P72R (c.215 C>G) heterozygous mutation in exon 4 of *TP53*.

ominous feature in many tumors. In respect to meningiomas, a number of studies suggest a correlation of p53 inactivation with histological tumor grade and risk of recurrence.^{13,14} However, the prognostic significance of Pro72Arg variation allele in meningiomas has not yet been determined.

The observation in the pediatric age group of a CNS tumor showing rhabdoid features mainly suggests the possible diagnosis of atypical teratoid/rhabdoid tumor. It

is a highly malignant embryonal tumor mostly affecting infants. Atypical teratoid/rhabdoid tumor typically has *INI-1* gene mutations.⁴ *INI-1* is a tumor suppressor gene located on chromosome 22q11.2 and its product, the INI-1 protein, is involved in chromatin remodeling.¹⁵ In our case, because of the young age of the patient, the possibility of an atypical teratoid/rhabdoid tumor was taken into consideration. Nevertheless, the immunohistochemical diffuse INI-1 nuclear positivity of the neoplastic cells and the absence of mutations of the *INI-1* gene excluded this possibility (*INI-1* mutations are not typical of rhabdoid meningioma¹⁴). Moreover, the tumor was completely negative to the glial and neuronal markers which are variably positive in atypical teratoid/rhabdoid tumor.⁴

With respect to the *NF2* gene, it is an oncosuppressor gene responsible for the hereditary syndrome neurofibromatosis 2. It encodes for merlin or schwannomin, proteins involved in the organization of membrane extensions and traffic and in cell growth, adhesion and signaling. Neurofibromatosis 2-associated meningiomas and about 60% of sporadic meningiomas are caused by mutation and/or deletion of the *NF2* gene.^{16,17} In our case, with the limitations of the method of study (RT-PCR), we could not substantiate a possible *NF2* gene inactivation.

In summary, although infrequent, rhabdoid meningiomas can occur in children. Owing to its rarity, each new case should be recorded to produce a better clinical, pathological, molecular, prognostic and therapeutic characterization of this lesion.

REFERENCES

- Menon G, Nair S, Sudhir J, Rao BR. Childhood and adolescent meningiomas: a report of 38 cases and review of literature. *Acta Neurochir* 2009; **151**: 239–244.
- Caldarella A, Buccoliero AM, Marini M, Taddei A, Mennonna P, Taddei GL. Oncocytic meningioma: a case report. *Pathol Res Pract* 2002; **198**: 109–113.
- Gallina P, Buccoliero AM, Mariotti F, Mennonna P, Di Lorenzo N. Oncocytic meningiomas: cases with benign histopathological features and a favorable clinical course. *J Neurosurg* 2006; **105**: 736–738.
- Louis DN, Ohgaki H, Wiestler OD, Cavenee WK. *WHO Classification of Tumours of the Central Nervous System*, 4th edn. Lyon: IARC Press, 2007; 218–221.
- Germano IM, Edwards MSB, Davis RL, Schiffer D. Intracranial meningiomas of the first two decades of life. *J Neurosurg* 1994; **80**: 447–453.
- Perry A, Giannini C, Raghavan R *et al.* Aggressive phenotypic and genotypic features in pediatric and NF2-associated meningiomas: a clinicopathologic study of 53 cases. *J Neuropathol Exp Neurol* 2001; **60**: 994–1003.

7. Perry A, Scheithauer BW, Stafford SL, Abell-Aleff PC, Meyer FB. "Rhabdoid" meningioma: an aggressive variant. *Am J Surg Pathol* 1998; **22**: 1482–1490.
8. Kepes JJ, Moral LA, Wilkinson SB, Abdullah A, Llena JF. Rhabdoid transformation of tumor cells in meningiomas: a histologic indication of increased proliferative activity: report of four cases. *Am J Surg Pathol* 1998; **22**: 231–238.
9. Chaturvedi S, Dua R, Singhal S, Kumari R. Rhabdoid meningioma with cranial nerve involvement: case report of a child. *Clin Neuropathol* 2008; **27**: 248–251.
10. Nozza P, Raso A, Rossi A *et al*. Rhabdoid meningioma of the tentorium with expression of desmin in a 12-year-old Turner syndrome patient. *Acta Neuropathol* 2005; **110**: 205–206.
11. Martínez-Lage JF, Ferri Niguez B, Sola J, Pérez-Espejo MA, Ros de San Pedro J, Fernandez-Cornejo V. Rhabdoid meningioma: a new subtype of malignant meningioma also apt to occur in children. *Childs Nerv Syst* 2006; **22**: 325–329.
12. Cai C, Zhang Q, Shen C *et al*. Rhabdoid meningioma in a child: report of a case and literatures review. *Chin J Clin Oncol* 2008; **5**: 67–71.
13. Terzi A, Saglam EA, Barak A, Soylemezoglu F. The significance of immunoistochemical expression of Li-67, p53, p21, and p16 in meningiomas tissue arrays. *Pathol Res Pract* 2008; **204**: 305–314.
14. Yang SY, Park CK, Park SH, Kim DG, Chung YS, Jung HW. Atypical and anaplastic meningiomas: prognostic implications of clinicopathological features. *J Neurol Neurosurg Psychiatry* 2008; **79**: 574–580.
15. Perry A, Fuller CE, Judkins AR, Dehner LP, Biegel JA. INI1 expression is retained in composite rhabdoid tumors, including rhabdoid meningiomas. *Mod Pathol* 2005; **18**: 951–958.
16. Buccoliero AM, Gheri CF, Castiglione F *et al*. Merlin expression in secretory meningiomas: evidence of an NF2-independent pathogenesis? Immunohistochemical study. *Appl Immunohistochem Mol Morphol* 2007; **15**: 353–357.
17. Buccoliero AM, Castiglione F, Degl'Innocenti DR *et al*. NF2 gene expression in sporadic meningiomas: relation to grades or histotypes real time-pCR study. *Neuropathology* 2007; **27**: 36–42.